NUMERICAL ANALYSIS OF LOW-INTENSITY SCHOTTKY SPECTRA RECORDED AS TIME SERIES

F. Nolden, GSI, Darmstadt, Germany

Abstract

Schottky spectra of extremely well cooled low-intensity ion beams suffer from a low signal-to-noise ratio. Their digital post-processing is neither well prescribed nor trivial. The paper presents a comparison of the use of Hanning windows with overlapping samples on one hand, and of multitaper analysis, on the other hand. It is shown that the area under the Schottky peak is better defined if the multitaper method is used.

INTRODUCTION

Modern Spectrum spectrum analyzers nowadays usually offer several types of measurements. One of these measurement modes records the digitized data in the time domain after down conversion of the central frequency, as well as digital and analog filtering in a predetermined frequency span which is directly coupled to the sampling frequency. The digital data consist of in-phase and quadrature (IQ) components which are stored on disk. Because the data are stored without any gap in the time domain it is possible to analyze data packages of any desired size.

This article describes a set of first results which were gained with an RSA3303B analyzer from Tektronix. Two types of data evaluation are presented:

1. Evaluation using the classical averaging method with overlapping averages using a cosine (von Hann or Hanning) window.

2. Evaluation using the more advanced multitaper method.

MATHEMATICAL MODELLING OF SCHOTTKY SPECTRA

Single Particle Signal

The classical picture of Schottky spectra of coasting beams assumes a beam of N particles with constant revolution frequecies ω_n (or revolution periods $T_n = 2\pi/\omega_n$) which are positioned azimuthally in a random fashion. In order to take account of this position, one assumes a time lag τ_n, $0 \leq \tau_n < T_n$ for each particle. Any interaction among the particles or with other particles (internal gas jet target, cooling of any kind etc.) is neglected.

In the limit of an infitite number of passages through the Schottky probe, the Fourier transform of the resulting signal of each particle can be written

$$\tilde{U}(\Omega) = \frac{Z_L Q e \omega}{2} \sum_{m=-\infty}^{+\infty} S(\Omega) e^{-i\Omega\tau_n} \delta(\Omega - m\omega_n) \quad (1)$$

where $S(\Omega)$ is the Fourier transform of the sensitivity $s(t)$. The spectrum has peaks at every harmonic of the revolution frequency. As the phases $\omega_n\tau_n$ are random, one has to describe somehow its statictical properties.

Schottky Spectrum

The 'process' $U(t)$ is characterized by its autocorrelation function

$$R(t,\tau) = \langle U(t+\tau/2)U(t-\tau/2)\rangle \quad (2)$$

where $< \cdots >$ denotes a sample average. If the process $U(t)$ is stationary, then R is independent of t, i.e. $R(t,\tau) = R(\tau)$. The Fourier $S(\Omega)$ transform of $R(\tau)$ is then called the power spectrum of U. If the unit of U is volts, then $S(\Omega)$ has the unit $\mathrm{V}^2\mathrm{s}$. In the case of the Schottky spectrum, it is given by

$$S(\Omega) = \frac{N(Qe)^2}{m}\Psi(\Omega/m) \quad (3)$$

where $\Psi(\omega)$ is the revolution frequency distribution, assuming that there is no Schottky band overlap. It is assumed that $\Psi(\omega)$ is normalized to one.

Due to its statistical origin, the power spectrum can only be *estimated* from a single measurement.

ANALOG SIGNAL PROCESSING

Figure 1 shows how the analog signal from the Schottky pick-up is processed. The mixer can be modeled mathematically as a multiplier with the input signal U_i

$$U_n(t) \propto \cos(\omega_n t + \phi_n) = \cos\left((\omega_{\mathrm{LO}} + \delta\omega_n)\, t + \phi_n\right) \quad (4)$$

and the local oscillator (LO) signal

$$U_{\mathrm{LO}} \propto \cos(\omega_{\mathrm{LO}} t) \quad (5)$$

yielding signals at $\omega_i \pm \omega_{\mathrm{LO}}$. If this is done by using first the LO frequency directly and secondly after a 90 degree phase shift, one gets the in-phase (I) and quadrature phase (Q) low-frequency signals

$$U_I \propto \cos(\delta\omega_n t - \phi_n) \quad (6)$$

$$U_Q \propto \sin(\delta\omega_n t - \phi_n) \quad (7)$$

If both signals are available, one can decide which parts of the low frequency signal arise from rf components at either $\omega_{\mathrm{LO}} + \delta\omega_n$ or $\omega_{\mathrm{LO}} - \delta\omega_n$. This can be done either by using another 90 degree shift of the quadrature signal and adding or subtracting this signal from the in phase signal (image reject mixer) or by digitizing both signals and treat them numerically as a complex number $U_I + iU_Q$. After a digital Fourier transform (DFT) one gets different components below and above zero frequency.

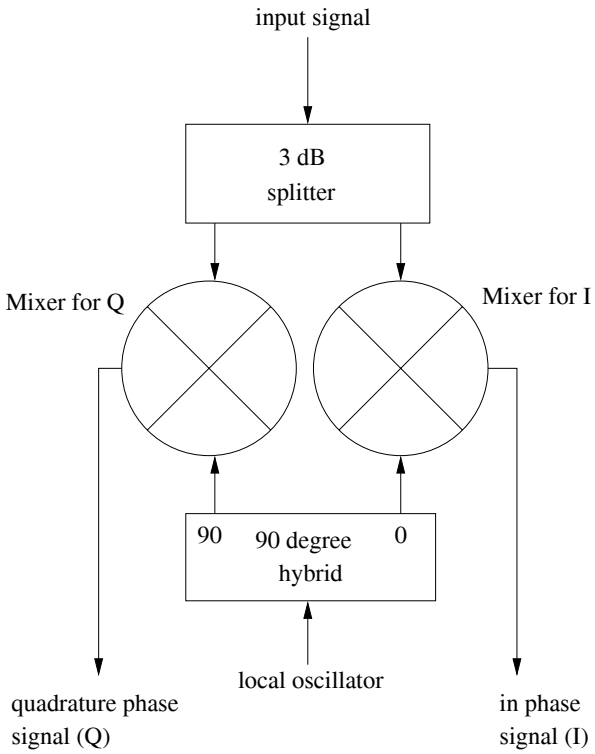

Figure 1: Signal processing in vector spectrum analyzer IQ mixer.

DIGITAL SPECTRUM ANALYSIS

We assume a digital complex dataset U_n, $0 \leq n < N-1$, sampled at a rate $1/\Delta t$. In the frequency domain this corresponds to a spectrum $\tilde{U}_n$ with frequency steps $\delta f = 2N/\Delta t$ The digital signal has two essential drawbacks, which may lead to problems:

1. It is of finite length, leading to spectral leakage, which can be overcome by tapering at the expense of spectral resolution.

2. It is sampled at a finite rate, which limits the spectral width and can cause aliasing.

While aliasing can normally be overcome by using a sufficiently high number of points in the DFT, the effect of leakage is more difficult to handle.

Leakage occurs because the measurement time interval T is finite. If an infinite set of measurements is cut abrubtly, one can represent the resulting frame as the product of the infinite set with a rectangular function. In the frequency domain this is equivalent to performing a convolution of the Fourier transform of the time series with a $\sin(\Omega T/2)/\Omega$ function which would cause sidelobes around every sharp frequency.

These sidelobes must be decreased by windowing. One multiplies the time series U_i with a series exhibiting w_n soft edges.

$$U_n \mapsto U_n w_n \tag{8}$$

A typical window used is the so called Hanning window (a name that was introduced in the anglo-saxon literature in order to refer to a German engineer called von Hann).

$$w_n = h_n = \left(\frac{2}{3(N+1)}\right)^{1/2}\left[1-\cos\left(\frac{2\pi n}{N+1}\right)\right] \tag{9}$$

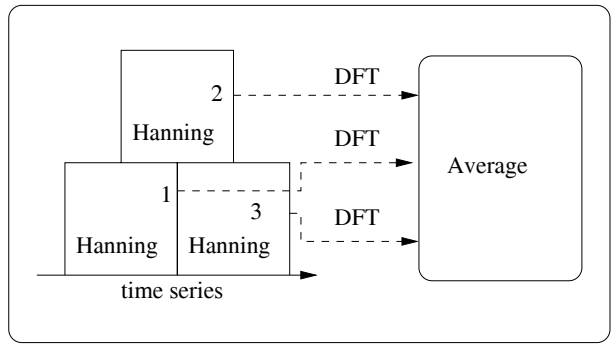

Overlapping Sample Averaging

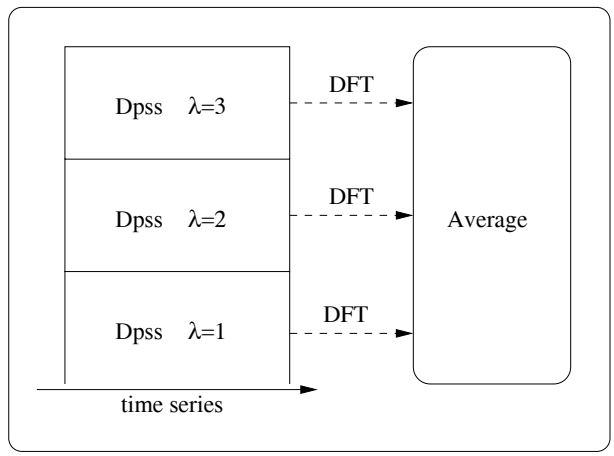

Multitaper Averaging

Figure 2: Overlapping sample averaging versus multitaper averaging.

Overlapping sample averages

Because windowing is equivalent to throwing away data at the edges of the time series one can use overlapping samples in order to include all of the data.

For each sequence U_i one gets the spectral estimate

$$S_j = \left|\sum_{n=0}^{N-1} U_n w_n \exp\left(-2\pi i j\right)\right|^2 \tag{10}$$

If one is not interested in temporal resolution, it is a common practice to average over these overlapping samples. An averaged estimate can be caculated by taking the mean over single overlapping sequence estimates. In the following we call this kind of averaging Walsh overlapping sample averages (wosa, according to the textbook [1]), although we do not use any explicit averaging.

Multitaper Analysis

In contrast to overlapping averages, the multitaper method [1] uses orthogonal sequences $v_{n,k}$ as tapers on the same finite dataset:

$$\sum_n v_{n,k} v_{n,l} = \delta_{k,l} \tag{11}$$

In particular one uses the DPSS tapers (Disctrete Prolate Spheroidal Sequences) $v_{n,k}(W)$, which are eigensolutions to the eigenvalue equation

$$\sum_{n=0}^{N-1} \frac{\sin\left(2\pi W(n-m)\right)}{\pi(n-m)} v_{n,k}(W) = \lambda_k(W) v_{m,k}(W) \tag{12}$$

with eigenvalue $\lambda_k(W)$. These sequences depend on a parameter W called the resolution bandwidth. The decisive property of DPSS sequences is that their use as windows minimizes spectral leakage. The spectral estimate is then calculated using the average

$$S_m = \sum_{k=0}^{K-1} \left| \sum_{n=0}^{N-1} U_n v_{n,k} e^{2\pi i n m} \right|^2 \tag{13}$$

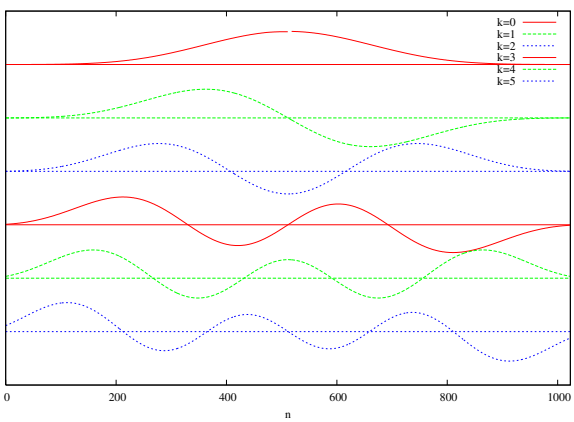

Figure 3: Series of DPSS tapers.

Figure 3 shows the DPSS tapers used in this paper with $N = 1024$ and the bandwidth parameter $W = 4/N$. This bandwidth appears to be an optimum choice for the simplification of peak identification. The tapers are numbered towards decreasing eigenvalues $\lambda_k(W)$, i.e. the $k = 0$ taper is the one with the largest eigenvalue. Multitapering has some remarkable features:

- The tapers can be non-zero (except for $k = 0$).
- Whereas the $k = 0$ taper is non-zero only in the middle of the time series, the following tapers more and more approach its edges. The $k = 5$ taper is even non-zero at the edges, which leads to some spectral leakage.
- Because the edges are used, the information contained in the time series is used effectively, in contrast to singe windowing where the information at the edges is effectively thrown away.
- Because the tapers are orthogonal, the spectra used in the averaging process are independent.

The tapers shown in Figure 3 have been calculated from a recipe presented in chapter 8 of [1], where a different eigenvalue equation by Slepian [2] is used with a tridiagonal matrix which has to be inverted. Furthermore the different eigenvectors are calculated by forced orthogonalization.

COMPARING SPECTRAL ESTIMATES WITH DIFFERENT EVALUATION ALGORITHMS

Figure 4 shows two spectral series calculated from identical time domain data. These data were measured at the 30^{th} harmonic (59.220875 MHz) of the Schottky spectrum of a 1 nA beam of $^{40}Ar^{18+}$ ions (about 180 particles) at an energy of 400 MeV/u. The momentum spread was reduced by electron cooling to extremely low values (see [3], [4] and [5]). The spectra on the left-hand side are single spectra with Hanning windowing and 50 % overlap. The spectra are taken from records (sometimes also called frames) in the time domain containing 1024 points. The distance between independent (non-overlapping) records is 128 ms.

The spectra on the right-hand side were calculated from the same data using the multitaper method with the first six of the $N = 1024$, $W = N/4$ tapers as presented in the previous section. Because there is no overlap, the number of spectra on the left-hand side is roughly twice as large as on the right-hand side.

In both cases one can see in many spectra a distinct peak at frequencies around 59,330,875 MHz. However, there are also many cases where the peak seems to hop or to be smeared out. The physical reason of this behaviour is not yet very clear. In any case, it leads to a substantial difficulty in interpreting such spectra. It is therefore crucially important to have meaningful spectral estimates.

When comparing both estimates, one has the impression that the peaks are somwhat better distinguished in the multitaper estimates. This impression can be confirmed numerically. To this purpose the area under the peak in an interval with a span of 10 Hz was determined and the background was subtracted. These areas are shown in figure 5.

It is visually obvious that the variation of the curve areas from the multitaper estimates is less than the variation due to the wosa estimates. Table 1 shows the average peak area $< F >$, its standard deviation $\sigma(F)$ and the relative deviation $\sigma(F)/ < F >$. Obviously for the wosa spectra the standard deviation is roughly as large as the mean value, for the multitaper estimates the standard deviation is two-thirds of the mean value.

One can therefore conclude that an evaluation using multitapers is superior to the usual overlapping sample es-

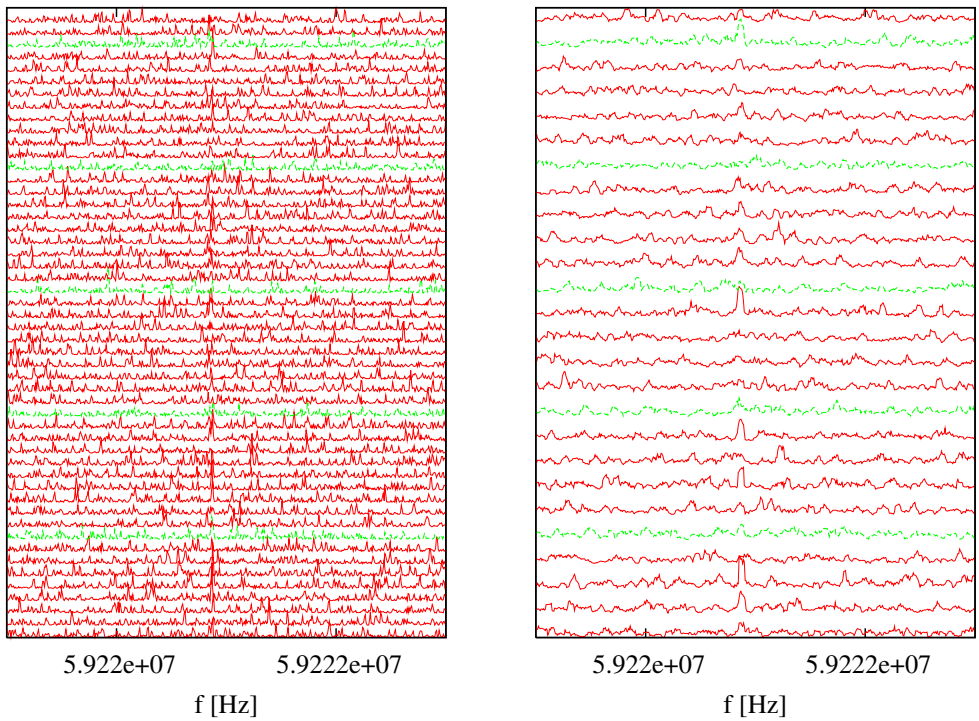

Figure 4: Estimated spectra with Hanning window and 50% overlap (left) and multitapering without overlap (right).

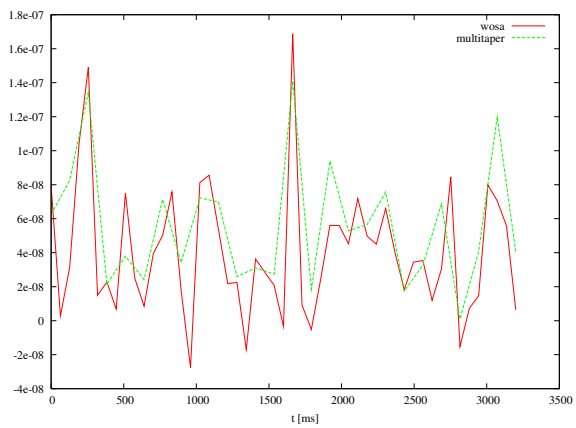

Figure 5: Calculated peak areas with wosa and multitapering.

timates with Hanning windows. Furthermore it should be noted that the spectra seem to feature intrinsic shifts or temporary heating effects, which prevent a smaller $\sigma(F)/ < F >$ value.

Table 1: Basic Parameters of the CR

	$< F >$	$\sigma(F)$	$\sigma(F)/ < F >$
wosa	$4.05 \cdot 10^{-8}$	$3.85 \cdot 10^{-8}$	0.95
multitaper	$5.60 \cdot 10^{-8}$	$3.64 \cdot 10^{-8}$	0.65

REFERENCES

[1] D. B. Percival, A. D. Walden, Spectral Analysis for Physical Applications, Cambridge University Press 1993

[2] D. Slepian, Prolate Spheroidal Wave Functions, Fourier Analysis, and Uncertainty, *Bell System Technical Journal*, **57**, 1371-1430

[3] M. Steck, K. Beckert, H. Eickhoff, B. Franzke, F. Nolden, H. Reich, B. Schlitt, T. Winkler, Anomalous Temperature Reduction of Electron Cooled Heavy Ion Beams in the Storage Ring ESR, *Phys. Rev. Lett.*, **77** (1996), 3803

[4] M. Steck, K. Beckert, P. Beller, B. Franzke and F. Nolden, New evidence for one-dimensional ordering in fast heavy ion beams, *J. Phys. B: At. Mol. Opt. Phys*, **36** (2003), 991-1002.

[5] M. Steck, P. Beller, K. Beckert, B. Franzke and F. Nolden, Electron Cooling Experiments at the ESR,
Nucl. Inst. Meth. A, **532** (2004), 357-365

[6] Yu.A. Litvinov et al., Observation of Non-Exponential Electron Capture of Hydrogen-Like ^{140}Pr and ^{142}Pm ions *Physics Letters B*, **664**, Issue 3, 162-168.